

# Addition Reactions of $^1\text{D}$ and $^3\text{P}$ Atomic Oxygen with Acetylene. Potential Energy Surfaces and Stability of the Primary Products. Is Oxirene Only a Triplet Molecule? A Theoretical Study

Yvan Girard and Patrick Chaquin\*

Laboratoire de Chimie Théorique, UMR 7616 Université Pierre et Marie Curie-CNRS, Box 137, 4, Place Jussieu, 75252 Paris Cedex 05, France

Received: August 27, 2002; In Final Form: June 12, 2003

The potential energy surfaces (PES) of the primary addition reactions of atomic oxygen  $\text{O}(^1\text{D})$  and  $\text{O}(^3\text{P})$  on acetylene were done using Density Functional Theory with the standard B3LYP hybrid functional. The crucial areas of these PES were then refined using the UMP2 and CCSD(T) schemes and, in few cases, CASPT2, MCSCF, and MR-AQCC ones. The stability of these primary products was studied. The reactivity of  $\text{C}_2\text{H}_2$  and O, especially in low-temperature matrix conditions, is discussed on these bases. The singlet surface shows that the insertion of the oxygen into the C–H bond, resulting in ethynol  $\text{HC}\equiv\text{COH}$ , is the main reaction. An addition onto the  $\text{C}\equiv\text{C}$  bond, leading to oxirene and/or formylcarbene  $\text{HC}-\text{CHO}$  is nevertheless to be considered. A particular attention was given to the oxirene-formylcarbene region and MR-AQCC calculations predict an extremely flat area in agreement with previous CCSD(T) results. Secondary transposition of formylcarbene into ketene  $\text{H}_2\text{C}=\text{C}=\text{O}$  could be avoided at very low temperature. From the triplet state of the oxygen atom, the triplet formylcarbene is expected as the major product. Nevertheless, a cyclic nonplanar species, the triplet state of oxirene, is stable on the triplet surface and could be trapped at low temperature, provided an intersystem triplet singlet crossing does not occur, which would lead to singlet oxirene, if stable. If not, this process would lead to singlet formyl carbene and finally to its triplet ground state. Indeed, singlet and triplet surfaces are very close to one another in this part of the PES. Hydrogen transposition giving triplet ketene can be ruled out in matrix conditions. The formation of cyclic three-member carbenes  $-\text{C}-\text{O}-\text{CH}_2-$ , as well singlet as triplet, is unlikely though both species are rather stable on their respective PES.

## 1. Introduction

Reactions of atomic oxygen with small organic compounds have brought forth numerous theoretical and experimental studies. The triplet ground-state  $\text{O}(^3\text{P})$  has been the subject of many of them, in reactions with diatomic systems ( $\text{H}_2$ ,<sup>1</sup>  $\text{HCl}$ ,<sup>2</sup> etc.) or small polyatomic molecules.<sup>3–6</sup> The highly reactive singlet oxygen  $\text{O}(^1\text{D})$  also raised a lot of attention. Its reactions with  $\text{H}_2$ ,<sup>1,7</sup>  $\text{HCl}$ ,<sup>8</sup>  $\text{N}_2\text{O}$ ,<sup>9,10</sup> saturated hydrocarbons,<sup>11–13</sup> fluoroethane,<sup>14</sup> ethylene,<sup>13</sup> etc., have been studied experimentally and theoretically and were simulated with quasiclassical trajectories (QCT).<sup>7,10</sup> In the gas phase, most of these studies show that the reactions often end in bond breakings and production of radical moieties.

The present work treats the reaction of atomic oxygen on acetylene  $\text{C}_2\text{H}_2$ , a molecule found in atmosphere chemistry,<sup>15,16</sup> interstellar clouds,<sup>17</sup> and playing an important role in most hydrocarbon flames.<sup>18–21</sup>

As far as we know, no experimental or recent theoretical study of a singlet  $^1\text{D}$  oxygen atom on acetylene is available in the literature, though, in a pioneering work, most of the isomerization reactions of the  $\text{C}_2\text{H}_2\text{O}$  species have been studied by Tanaka.<sup>23</sup> Some parts of the  $\text{C}_2\text{H}_2\text{O}$  singlet PES have nevertheless been extensively studied from different points of view. First, oxirene, which has not yet been observed experimentally, gave rise to a number of calculations at various levels.<sup>22–24,31–33</sup> Second, the modeling of the Wolff rearrangement which consists of the transposition of a ketocarbene  $\text{CR}-\text{CH}=\text{O}$  into ketene

$\text{O}=\text{C}=\text{CHR}$  has been studied,<sup>23,28,32</sup> as well as the isomerization of ketene<sup>25</sup> resulting in a carbon atom exchange, which involves an oxirene intermediate. The singlet–triplet separation for a variety of formylcarbenes has been calculated.<sup>28</sup> Ethynol<sup>22–23,27</sup> has been characterized, and the reaction path of its isomerization into ketene has been studied theoretically.<sup>23</sup>

Several studies of the gas-phase reaction of triplet oxygen on acetylene are available.<sup>18–21</sup> A first channel consists of hydrogen abstraction yielding OH and CCH. A second one involves the addition intermediate  $\text{OC}_2\text{H}_2$  which dissociates into  $\text{H} + \text{OCCH}$ , or undergoes a transposition to yield  $\text{CH}_2 + \text{CO}$ . In these conditions neither the energy-rich addition intermediate, nor its possible isomerization products could be observed. The potential energy surfaces corresponding to the preceding reactions were calculated at the CISD level with a double  $\zeta$  basis set<sup>19</sup> and used for the determination of reaction rates.

On the other hand, atomic oxygen reactions can be carried out in inert gas matrixes at low temperature. Triplet or singlet atomic oxygen is easily generated, for example, by photolysis of ozone. This way, addition or insertion primary products can be trapped, unless they are highly reactive, and can be studied by spectroscopic methods. This technique has been successfully used with a variety of substrates such as  $\text{CH}_4$ ,  $\text{CH}_3\text{OH}$ ,<sup>53</sup>  $\text{CCl}_3-\text{CH}_3$ ,<sup>54</sup> or  $\text{CH}_3\text{OCH}_3$ .<sup>55</sup> Moreover, it allowed us to characterize them as labile species as XOY and XYO ( $\text{X},\text{Y} = \text{Cl}, \text{Br}$ ).<sup>56</sup>

Our contribution is, in a first step, a presentation of the comprehensive potential energy surfaces (PES) of the  $\text{O}(^1\text{D}) + \text{C}_2\text{H}_2$  and  $\text{O}(^3\text{P}) + \text{C}_2\text{H}_2$  reactions at the UB3LYP/6-31G\*\* level which gives an insight on the reactivity and the nature of primary

\* To whom correspondence should be addressed.

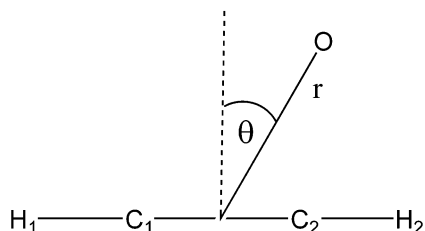


**Figure 1.** Definition of the main parameters  $r$  and  $\theta$  used for PES calculations of Figures 2, 3, 8, and 9.

products. In a second step, a systematic study of these primary products, of their stability, and of their isomerization has been done at reliable calculation levels. We focused our attention on possible formations of unknown species such as oxirene or transient such as carbenes or diradicals which could be trapped at low temperatures. We have taken into account possible intersystem crossing by calculating singlet–triplet separation in some crucial areas of the PES.

Though we will not study further possible cleavages, we can nevertheless offer a useful guideline for the main trends of the gas-phase singlet reactivity, which has not yet been studied experimentally, as compared with the triplet one.

## 2. Methodology

The potential energy surfaces (PES) of the reactions  $\text{O}(^1\text{D}) + \text{C}_2\text{H}_2$  and  $\text{O}(^3\text{P}) + \text{C}_2\text{H}_2$  were computed using, as a first approach, unrestricted density functional theory (UDFT) with the Becke's three parameters hybrid functional UB3LYP<sup>34</sup> and Pople 6-31G\*\* basis set. Unrestricted DFT was chosen to account for hypothetical open shell species as it has been done with success in several open-shell singlet problems.<sup>35</sup> Though the singlet system should be poorly described by this method at infinite  $\text{O}-\text{C}_2\text{H}_2$  separation because of its 5-fold degeneracy, we checked that the use of this single configuration is relevant in the parts of the PES of interest for reactivity purposes. As a matter of fact, on one hand, the values of  $S^2$  remain very close to the expected value of 0; on the other hand, a multiconfiguration (MC) calculation indicated that the lowest state consists of a single configuration, by more than 80%, when the distance between both entities is less than 2.5 Å. Two main geometric parameters were selected (Figure 1): the distance  $r$  between the oxygen atom and the center of the CC bond, and the angle  $\theta$  between the perpendicular to the CC bond and the  $r$  segment. We calculated an array of potential energy curves with frozen angles  $\theta$  (from  $0^\circ$  to  $90^\circ$  by steps of  $2^\circ$ ) and varying distance  $r$  from 4 to 0.5 Å. All of the remaining parameters were optimized at each point of this scan. Finally, the potential energy curves were gathered to build up the surfaces, assuming therefore the continuity between them.

The surfaces were first checked by recomputing the stationary points at the same level of calculation. Then, stationary points were calculated, and small portions of the surface were rescanned at the higher levels of calculations Møller–Plesset (MP2) and coupled cluster theory with perturbative inclusion of triple excitations (CCSD(T)).<sup>36</sup> In some cases, complete active space plus second-order perturbation theory (CASMP2) and multireference average quadratic coupled cluster (MR-AQCC),<sup>37–39</sup> a modified multireference configuration interaction (MR–CI) procedure was used. The Pople diffuse basis set 6-311++G\*\* was used for MP2 calculations, whereas CCSD(T), CASMP2, and MCSCF/MR-AQCC results were obtained with the correlation-consistent Dunning cc-pVTZ basis set.<sup>40</sup> Single reference calculations (DFT, MP2, and CCSD(T)) were

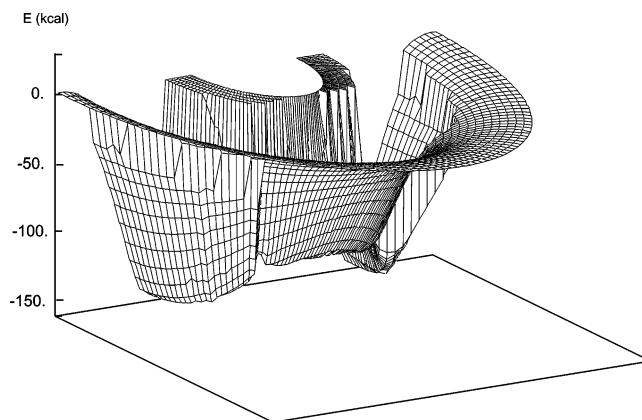


**Figure 2.** Potential energy (kcal/mol) surface of the reaction of atomic oxygen ( $^1\text{D}$ ) on acetylene. See also Figure 3.

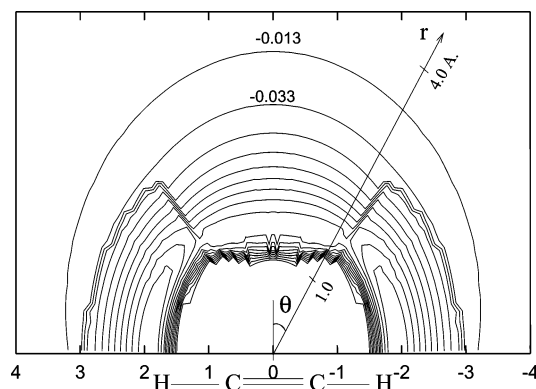


**Figure 3.** Isoenergy curves of the reaction of atomic oxygen ( $^1\text{D}$ ) on acetylene (planar projection of Figure 2 PES) by steps of 0.02 ua; values reported with respect to asymptotic energy; distances in angstroms and angles in degrees.

**TABLE 1: Energies of the Singlet Species (Hartrees)**

	UB3LYP <sup>a</sup>	UMP2 <sup>b</sup>	MR-AQCC <sup>c</sup>	CCSD(T) <sup>d</sup>
<b>1</b>	-152.47738	not found	-152.21606	-152.23394 <sup>e</sup>
<b>2</b>	-152.53905	-152.18065		-152.30399
<b>3</b>	-152.47014	-152.10587	-152.21509	-152.23226
<b>5 TS</b>	-152.44388	-152.08083	-152.18747	-152.20370 <sup>f</sup>
<b>6</b>	-152.60203	-152.23546		-152.35818
<b>6c</b>	-152.50230	-152.13213		-152.26259
<b>7 TS</b>	-152.46909	-152.09299		-152.22594 <sup>f</sup>

<sup>a</sup> 6-31G\*\*, <sup>b</sup> 6-311++G\*\*, <sup>c</sup> cc-pVTZ, CAS(8,7) geometry, <sup>d</sup> cc-pVTZ, <sup>e</sup> UDFT geometry, <sup>f</sup> UMP2 geometry.

performed using the Gaussian 98 package;<sup>41</sup> MCSCF, CASMP2, and MR-AQCC calculations were carried on with the MOLPRO (2000.4) series of programs.<sup>42–44</sup>

## 3. Reactivity of Singlet Oxygen Atom $\text{O}(^1\text{D})$ on Acetylene

**3.1. General Scope of the Potential Energy Surface (UB3LYP/6-31G\*\*).** The 3-dimensional surface is shown in Figure 2 and its projection in Figure 3. Energies of the different singlet species (described in Figure 4) are shown in Table 1, and geometries are gathered in Tables 2 and 3. Figure 5 shows the relative energies of the discussed compounds. From the DFT surface of Figures 2 and 3, three comments can be made.

(i) A first couple of minima are observed ( $\theta = \pm 32.9^\circ$  and  $d = 1.5$  Å) corresponding to singlet formylcarbene (or formylmethylene) **1**, by formation of a  $\text{C}=\text{O}$  bond. The more stable conformation is nonplanar: a skewed structure allows a donation from the oxygen lone pair to the carbene empty p orbital. This species has been predicted theoretically<sup>23,24,28</sup> but has still to

**TABLE 2: Calculated Geometries (Lengths in Angstroms, Angles in Degrees) of Singlet Formylcarbene 1, Oxirene 3, and Isomerization TS 5 and 7<sup>a</sup>**

		C <sub>1</sub> C <sub>2</sub>	C <sub>1</sub> H <sub>1</sub>	C <sub>2</sub> H <sub>2</sub>	C <sub>1</sub> O	OC <sub>1</sub> C <sub>2</sub>	H <sub>1</sub> C <sub>1</sub> C <sub>2</sub>	C <sub>1</sub> C <sub>2</sub> H <sub>2</sub>	OC <sub>1</sub> C <sub>2</sub> H <sub>2</sub>	OC <sub>1</sub> C <sub>2</sub> H <sub>1</sub>
<b>1</b>	UDFT	1.370	1.095	1.091	1.264	95.9	136.8	120.2	-80.4	169.8
	MR-AQCC <sup>b</sup>	1.383	1.078	1.081	1.257	91.0	141.0	114.2	-85.9	173.0
<b>3</b>	UDFT	1.268	1.073	1.073	1.504	65.1	161.8	161.8	180.0	180.0
	UMP2	1.248	1.033	1.048	1.564	66.5	161.4	161.8	180.0	180.0
	MR-AQCC <sup>b</sup>	1.265	1.059	1.059	1.512	65.3	160.2	160.2	180.0	180.0
	CCSD(T)	1.275	1.070	1.070	1.502	64.9	161.9	161.9	180.0	180.0
<b>5 TS</b>	UDFT	1.238	1.177	1.064	1.295	176.2	106.0	170.4	0.0	0.0
	UMP2	1.246	1.178	1.064	1.276	170.1	96.5	174.5	0.0	0.0
<b>7 TS</b>	UDFT	1.417	1.128	1.103	1.229	125.4	110.8	114.4	-93.5	173.2
	UMP2	1.442	1.115	1.103	1.228	121.0	115.4	110.2	-90.7	174.4

<sup>a</sup> See caption of Table 1 for more detail. <sup>b</sup> Geometry taken from a scan of Figure 7.

**TABLE 3: Calculated Geometry (Lengths in Angstroms, Angles in Degrees) of the Ethynol 2**

	HC	CC	CO	OH	HCC	CCO	COH	HOCC	OCCH
UDFT <sup>a</sup>	1.063	1.206	1.315	0.969	179.4	176.8	109.6	180.0	180.0
UMP2 <sup>b</sup>	1.062	1.214	1.315	0.964	179.4	176.5	108.3	180.0	180.0
CCSD(T) <sup>c</sup>	1.061	1.208	1.319	0.964	179.8	176.7	108.5	180.0	180.0

<sup>a</sup> 6-31G\*\*, <sup>b</sup> 6-311++G\*\*, <sup>c</sup> cc-PVTZ.

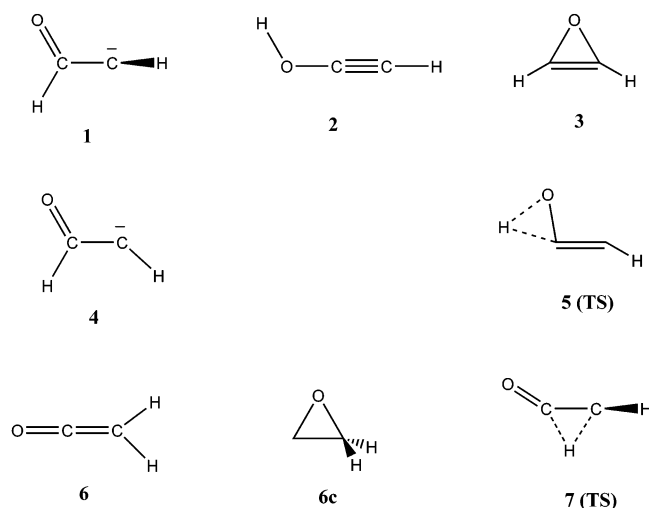


**Figure 4.** C<sub>2</sub>H<sub>2</sub>O singlet species; **5** is the TS linking **2** to **1** or **3**; **7** is the TS linking **1** and **6**.

be observed experimentally though its lifetime has been recently studied by laser flash photolysis<sup>29</sup> and transient grating spectroscopy.<sup>30</sup> The formylcarbene has a triplet ground state, with a planar geometry. Nevertheless, the singlet state is indeed involved during the Wolff reaction; therefore, the triplet-singlet gap is quite narrow. This point will be discussed in section 4.3.

(ii) A second and lower couple of minima ( $\theta = \pm 87.6^\circ$  and  $d = 1.92 \text{ \AA}$ ) corresponds to the ethynol molecule **2**, arising from the insertion of the oxygen atom into a C-H bond. This species has been observed in a few experimental studies<sup>45,46</sup> and has been studied theoretically as the tautomer of ketene<sup>22,23</sup> or for its gas-phase acidity.<sup>26,27</sup> The Figure 2 PES indicates that ethynol is ca. 150 kcal/mol below the reactants C<sub>2</sub>H<sub>2</sub> + <sup>1</sup>O. Taking into account the constraints brought by the construction of the surface, the transition state connecting the species **1** and **2** was searched with a standard optimization method. The structure found **5** is indeed very close to the one observed on the surface. The corresponding energy barrier for a formylcarbene to ethynol isomerization is about 21 kcal/mol (see Figure 5).

(iii) At this level of calculation, no minimum is observed for the oxirene **3** which thus is not predicted as a stable compound. Because this prediction has been proved to be strongly dependent on the method used,<sup>31-33</sup> this point will be discussed more

**TABLE 4: Calculated Geometry (Lengths in Angstroms, Angles in Degrees) of the Ketene 6 and Cyclic Carbene 6c**

		C <sub>1</sub> C <sub>2</sub>	C <sub>1</sub> H	C <sub>2</sub> O	HC <sub>1</sub> C <sub>2</sub>	C <sub>1</sub> C <sub>2</sub> O <sub>2</sub>	HC <sub>1</sub> C <sub>2</sub> O
<b>6</b>	UDFT	1.322	1.080	1.168	119.1	180.0	
	UMP2	1.314	1.082	1.171	119.7	180.0	
<b>6c</b>	UDFT	1.514	1.085	1.283	120.0	62.8	92.7
	UMP2	1.516	1.082	1.287	119.8	63.7	94.5

carefully later on. At any rate, this surface emphasizes the possibility of an easy migration of the oxygen atom from one carbon to another via the oxirene structure before the strongly exothermic transposition into ketene, as it has been shown by <sup>13</sup>C labeling experiments<sup>47</sup> designed to understand the Wolff rearrangement.

**3.2. Further Calculations: Stability of Oxirene, Formylcarbene, and Ethynol. Interconversion Processes.** To obtain more reliable energy values, the stationary points on the PES have been calculated using more sophisticated methods. Energies and geometries are gathered in Tables 1-4. Relative energies for the different levels of theory are shown in Figure 5.

**Oxirene-Formylcarbene System.** At the UMP2/6-311++G\*\* level (see Figure 5), the geometry optimization of the formylcarbene **1** leads to the C<sub>2v</sub> oxirene **3**, which is therefore predicted as the only stable species in the area. The ethynol **2** is found 46.9 kcal/mol below oxirene **3**, and transition state (TS) **5** linking **3** to **2** lies about 16 kcal/mol above **3**, in reasonably good agreement with the UB3LYP/6-31G\*\* results.

At the CCSD(T)/cc-PVTZ level (see Figure 5), because of the high calculation costs, we only optimized C<sub>s</sub> ethynol **2** and symmetry constrained C<sub>2v</sub> oxirene **3**. For the formylcarbene and the TS **5**, a single-point energy calculation was performed using respectively the DFT and MP2 geometries. One can see that the CCSD(T) method does not agree with the MP2 results because the formylcarbene **1** is now predicted as the only local minimum following the addition of the oxygen on the double bond. However, the energy difference with **3** is very small (1.05 kcal/mol). This is not a breakthrough: several studies were done to determine whether the oxirene was a minimum or not, but no answer was definitely given.<sup>24,31-33</sup> From several tenths of calculation methods compiled by Vacek et al.,<sup>32</sup> it results that oxirene is generally found as a minimum at the SCF, MP2, and most of the CCSD levels, depending on the basis set used, whereas at the DFT level, it is found as the transition state of oxygen transposition from one carbon to another in formylcar-

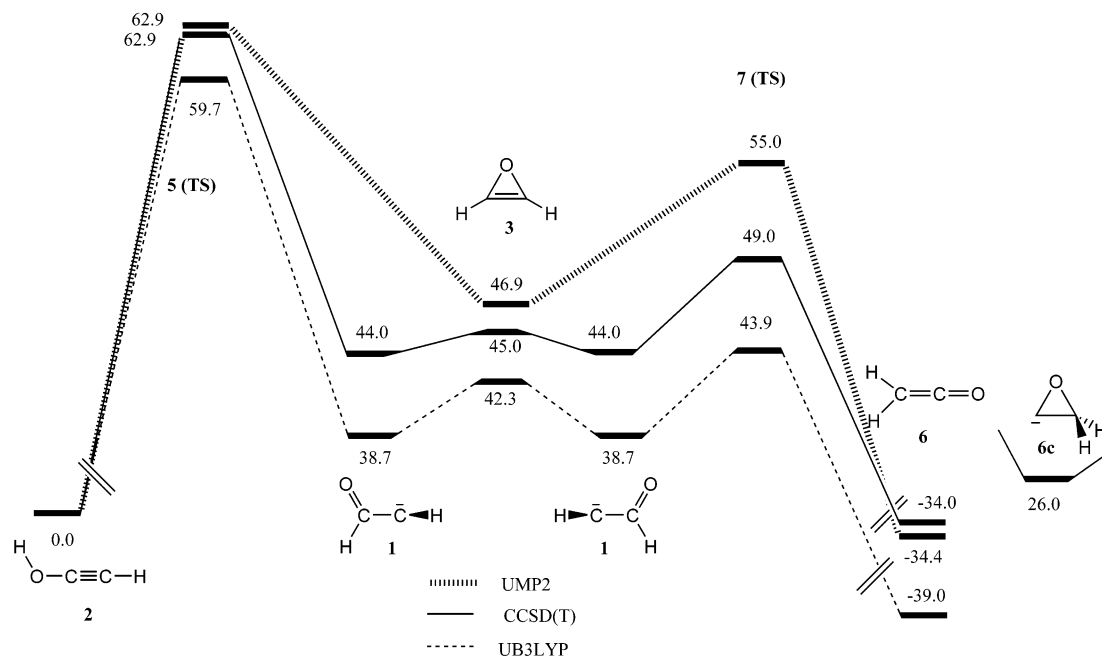


**Figure 5.** Energy profiles (kcal/mol) of singlet  $\text{C}_2\text{H}_2\text{O}$  species interconversion according to the calculation methods: UMP2/6-311++G\*\*, CCSD(T)/cc-pVTZ, and UB3LYP/6-31G\*\*.

bene. These results were confirmed by Scott et al.,<sup>24</sup> who calculated the PES of oxirene opening into formylcarbene using SCF, MP2, DFT, and finally CCSD(T)/cc-pVTZ calculations including f functions. At this latter level, oxirene was found as a minimum, separated from formylcarbene by a 0.4 kcal energy barrier (after ZPE correction). The authors concluded that it was not possible to state categorically on the nature of the stable species in this very flat part of the PES. These CCSD(T) results can be considered as very reliable as far as the system is mono-configurational. To check this point, we carried out MC calculations. As a matter of fact, the description of the CO bond breaking and, in a lesser extend, of the formylcarbene species could be a priori improved using multi-determinantal wave functions. Two methods including both dynamical and nondynamical correlation were used with the cc-pVTZ basis set: CASMP2 and MR-AQCC. The latter method is essentially a MR-CISD procedure modified toward size-extensivity and needed preliminary calculations: complete configuration sets were generated in active spaces containing 8 electrons in 7 natural orbitals. Lower orbitals were optimized but kept doubly occupied. Comparisons with larger and smaller spaces showed that this (8,7) space was a good compromise: at the MCSCF/cc-pVTZ level, calculations of the planar oxirene opening gave a potential energy curve close to the full valence MCSCF (16,14), unfortunately far too big for subsequent MR-AQCC calculations. The three lowest orbitals (1s) were defined as “core” orbitals whereas the next four orbitals were “closed”, i.e., out of the reference space, doubly occupied in all CSFs, but included in the dynamical correlation energy calculation through single and double excitations. A third set, the active space, included of course the  $\sigma$  and  $\sigma^*$  orbitals associated to the C–O bond, to deal with the oxirene–formylcarbene interconversion by the breaking of this bond. As an example, for nearly oxirene geometries, the leading configuration was

core orbitals:  $(1a')^2 (2a')^2 (3a')^2$  (1s orbitals of heavy atoms)

closed orbitals:  $(4a')^2 (5a')^2 (6a')^2 (7a')^2$  ( $\sigma_{\text{CH}}$ ,  $\sigma_{\text{CC}}$  and  $\sigma$  oxygen lone pair)

active orbitals:  $(8a')^2 (9a')^2 (1a'')^2 (2a'')^2 (3a'')^0 (10a')^0 (11a')^0$  (3  $\pi$  orbitals,  $\sigma_{\text{CO}}$  and  $\sigma^*_{\text{CO}}$ )

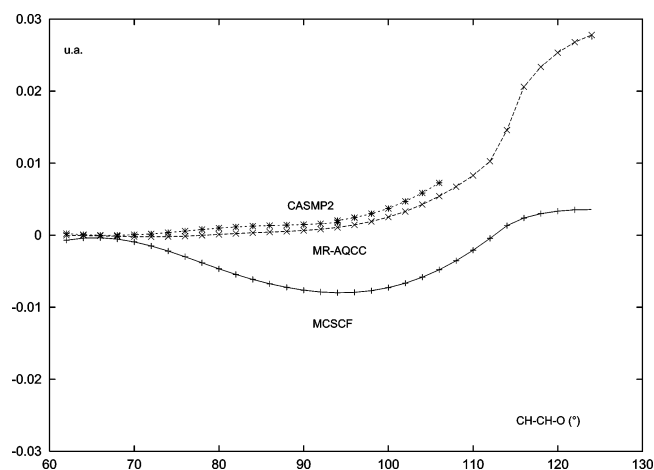


**Figure 6.** Potential energy (u.a.) curves of planar constrained opening of oxirene **3** as a function of the OC1C2 angle (deg) using various calculation methods. The MCSCF geometry has been used for other methods.

First, we scanned the planar ring opening of the oxirene according to this procedure by varying the CCO angle from  $62^\circ$  to  $128^\circ$  by  $2^\circ$  steps. All of the remaining parameters were optimized at the MCSCF (8,7) level, and CASMP2 or MR-AQCC energies were obtained afterward using this set of parameters. The resulting potential energy curves are shown in Figure 6, with symmetric oxirene taken as an arbitrary energy reference. Apparently, when the molecule is constrained to planarity, there is no minimum for an open species **4** and the oxirene **3** appears as a shallow minimum at both CASMP2 and MR-AQCC levels. It is worthy to note that at the MCSCF level the oxirene is no longer a minimum and an open form is predicted to lie 5 kcal/mol below.

Second, the same scan was performed while allowing the system to undergo out-of-plane deformation. The curves are shown in Figure 7. One can see that MCSCF calculations predict a spontaneous opening yielding the formylcarbene **1**. At the CCSD(T) and MR-AQCC levels, a very flat minimum is observed for the oxirene **3**, separated by a weak energy barrier



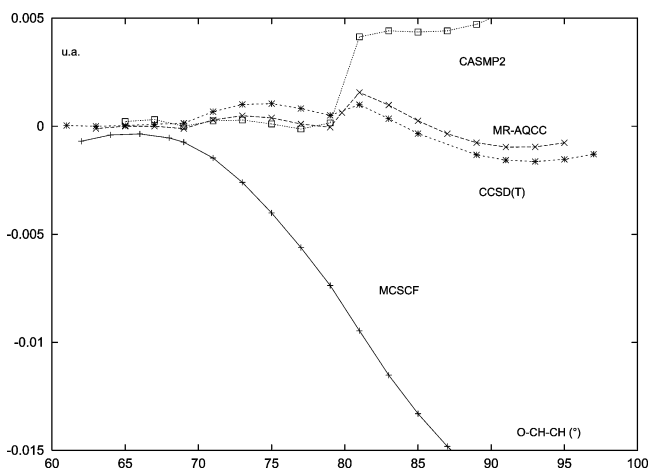


**Figure 7.** Potential energy (u.a.) curves of oxirene **3** opening into formylcarbene **1**, free of constraints, as a function of the OC1C2 angle (deg) using various calculation methods. The MCSCF geometry has been used for other methods.

(less than 1 kcal/mol) from another minimum corresponding to the formylcarbene **1** which lies 0.6–1 kcal/mol below **3**. At the CASMP2 level, the results (Figure 7) indicate a stable but very floppy oxirene and no minimum for the formylcarbene structure **1**. All three curves obtained at the highest level in Figure 7 exhibit a slight break at ca. 80°. As a matter of fact, the geometry used, optimized at the MCSCF level, is not fully optimal at the other levels because of a different coupling of the angle CCO taken as the main parameter with the HCCH dihedral angle. Let us nevertheless underline that this “jump” is less than 0.001 au at both CCSD(T) and MR-AQCC levels. Moreover, it was verified on one point (CCO = 90°) that the geometry optimization at the MR-AQCC level does not yield a significant improvement in energy. MR-AQCC energies and geometries found in Tables 1–3 are taken from those curves. From these results, two kinds of remarks can be drawn.

(i) From a technical point of view, a good description of this part of the PES appears to need an extensive treatment of the dynamical correlation. As a matter of fact, on one hand, MP2 and CASPT2 calculations do not predict a stable formylcarbene, and on the other hand, SCF, MCSCF, and DFT methods do not predict a stable oxirene. We can note that a nondynamical correlation tends to favor, as expected, open diradical/carbene structures with respect to the oxirene structure, but finally, the fact that CCSD(T) results are very close to MR-AQCC ones indicates the leading role of the dynamical correlation is this system.

(ii) From a chemical point of view, a qualitative prediction can be hardly done. At our best levels of calculation (MR-AQCC and CCSD(T)), both oxirene-like and carbene-like structures could exist, the latter being slightly more stable by 0.6–1 kcal/mol, in agreement with Scott et al.<sup>24</sup> At any rate, if one considers that the whole potential energy curve lies within about 1.5 kcal/mol, both oxirene and formylcarbene appear as very floppy species which, as far as they really exist, could be only trapped at very low temperatures. Finally, low-temperature formation of oxirene/formylcarbene would appear as the suitable method to answer this question by experimental means.

(iii) The planar opening of the oxirene is less easy, so a rigid molecule, forbidding an out-of-plane distortion, might favor an oxirene structure. Indeed, benzooxirene, for instance, has been predicted by theoretical means.<sup>48</sup>

**Formylcarbene–Ketene Interconversion.** As recalled in the Introduction, ketocarbenes CH–CR=O are key intermediates

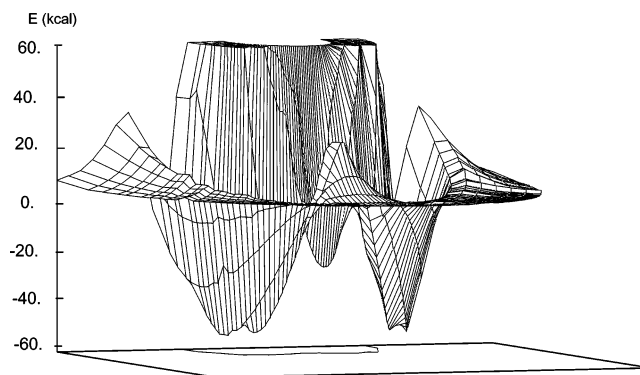


**Figure 8.** Potential energy (kcal/mol) surface of the reaction of atomic oxygen (<sup>3</sup>D) on acetylene. See also Figure 9.

in the Wolff rearrangement, which typically gives a ketene RHC=C=O from a diazoketone N<sub>2</sub>CH–CO–R. Numerous studies showed that, in the final step of the rearrangement, the system has to overcome a small energy barrier between the ketocarbene and the far more stable ketene.<sup>22–25</sup> In the case of the formylcarbene **1**, this barrier yielding ketene **6** is found at 5.2 kcal/mol (UB3LYP), 8.1 kcal/mol (UMP2), and 5.0 kcal/mol (CCSD(T)) very close to the value of 5.7 reported by Scott et al.<sup>24</sup> Therefore, at room temperature, the addition of the oxygen atom that would lead first to an oxirene/formylcarbene form is likely to end in a ketene, but at low temperatures, the latter step could be easily inhibited.

**Ethynol–Ketene Interconversion.** As pointed out from Figure 2, ethynol **2** is the most stable of the primary products, and it can be obtained without activation energy. Nevertheless, it is far less stable than its ketene tautomer **6**. A one-step isomerization of ethynol into ketene can be ruled out<sup>23</sup> because it involves a highly strained four-center TS. We thus have to consider a two-step process with formylcarbene as the intermediate. Because the latter species lies ca. 44 kcal/mol above ethynol, with an activation barrier ranging from 59.7 to 62.9 kcal/mol (see Figure 5), this process can be ruled out in low-temperature matrix conditions.

**Cyclic Form of Ketene.** The oxiranylidene cyclic carbene **6c**, of C<sub>s</sub> symmetry, which could result from a cyclization of ketene, can also be considered. This species is rather stable on the singlet PES, though it lies 26.0 kcal/mol above ethynol and 60.0 kcal/mol above ketene (at the CCSD(T) level). As a matter of fact, the frequencies of the vibrations associated to the ring opening are greater than 800 cm<sup>-1</sup>, indicating a marked local minimum in the PES. Nevertheless, its formation is very unlikely. In the TS **7**, the OC1C2 angle is about 125°, so that the system will evolve exothermally toward ketene **6** by increase of this angle, rather than give **6c** by decrease of this angle, which needs the overcoming of an additional energy barrier.

#### 4. Reactivity of Triplet Oxygen O(<sup>3</sup>P) with Acetylene

**4.1. General Scope of the Potential Energy Surface (UB3LYP/6-31G\*\*).** The UB3LYP/6-31G\*\* PES is shown in Figures 8 and 9. The energies and geometries of the discussed species (Figure 10) are gathered in the Tables 5–7. Examination of this PES deserves the following comments.

(i) The surface exhibits two deep minima for  $r = 1.7 \text{ \AA}$  and  $\theta = \pm 37^\circ$  corresponding to the addition of the oxygen atom on each carbon that leads to the triplet formylcarbenes **8** (trans) and **9** (cis). The cis form **9** is slightly higher in energy (less than 3 kcal/mol at UB3LYP/6-31G\*\*).

(ii) Another minimum ( $r = 1.2 \text{ \AA}$  and  $\theta = 0^\circ$ ) corresponds to the couple of species **10** and **11** of C<sub>s</sub> and C<sub>2</sub> symmetry,

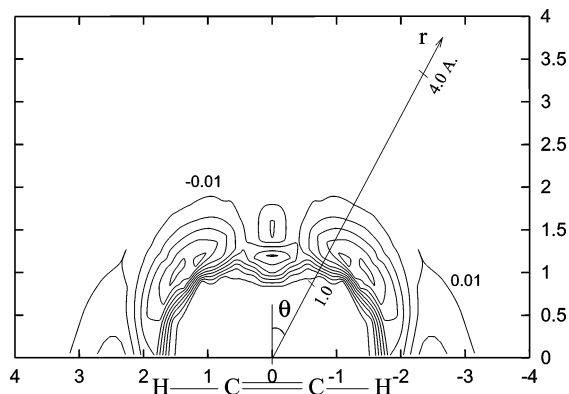


**Figure 9.** Isoenergy curves of the reaction of atomic oxygen ( $^3\text{D}$ ) on acetylene (planar projection of Figure 8 PES) by steps of 0.02 e.u.; values reported with respect to asymptotic energy; distances in angstroms and angles in degrees.

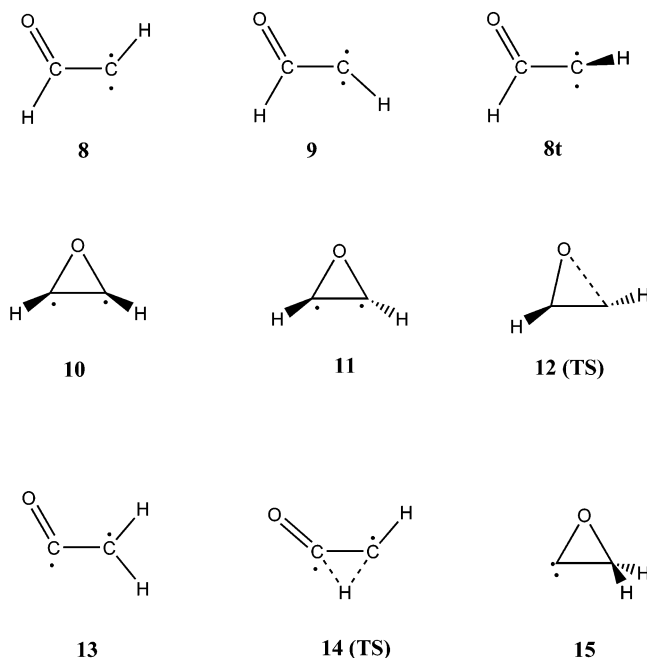


**Figure 10.**  $\text{C}_2\text{H}_2\text{O}$  triplet species; **8t** is the TS linking **8** and **9**; **12** is the TS linking **8t** to **11**; **14** is the TS linking **8** and **13**.

respectively. These are the lowest triplet  $\pi\pi^*$  state of oxirene **3**. As one can guess, the trans conformation is a little more stable than the cis one, because of the two even spin electron repulsion and interaction of hydrogen atoms. The closed trans form **11** lies 29.6 kcal/mol above the open structure **8**. The triplet PES shows that the well containing both of these species is apparently quite difficult to reach by a frontal  $C_{2v}$  attack ( $\theta = 0^\circ$ ) due to a high energy barrier that would probably push the oxygen back (about 20 kcal/mol). This barrier is much lower for  $\theta$  angles greater than  $0^\circ$ , but in this case, the system is more likely to fall down in the **8–9** well. Once obtained, **10** and **11** nevertheless appear to be quite stable on the triplet PES (the energy barrier toward the open form is predicted by the DFT to be about 30 kcal/mol).

**4.2. Further Calculations: Stability of Triplet Formylcarbene and Oxirene. Interconversion Processes.** The four structures **8–11** of the primary products have been optimized again at different levels of calculation. We considered, in addition, triplet ketene **13** and its cyclic form **15** as possible products of isomerization of **8–11**. Results are gathered in Tables 5–7. Relative energies and the reaction profile at the

CCSD(T)/cc-pVTZ//MP2/6-311++G\*\* level are displayed in Figure 11.

**Triplet Oxirene–Formylcarbene System.** All of the methods including extensive dynamic correlation give results very close to UB3LYP ones for the energy difference between the open structure **8** and the cyclic one **11**: 29.6 kcal/mol (UB3LYP), 28.1 kcal/mol (UMP2), 29.8 kcal/mol (MR-AQCC), and 28.2 kcal/mol (CCSD(T)). By contrast, a difference of 38.2 kcal/mol is found at the MCSCF(8,7) level.

The trans formylcarbene **8** is found slightly more stable than its cis isomer **9** by all of the calculation methods: 1.57 kcal/mol (UB3LYP), 1.03 kcal/mol (UMP2), 1.10 kcal/mol (MR-AQCC), and 1.23 kcal/mol (CCSD(T)). The **8–9** rotation through the TS **8t** needs to overcome an energy barrier of 6.06 and 6.85 kcal/mol at UMP2 and CCSD(T) levels respectively which could not be achieved at a very low temperature (e.g., 10 K). Similarly, the trans triplet oxirene **11** is found below its cis isomer **10**, but the energy difference is very small: 0.20 kcal/mol (UB3LYP), 0.68 kcal/mol (UMP2), 0.45 kcal/mol (MR-AQCC), and 0.43 kcal/mol (CCSD(T)).

The reaction coordinate linking **8–11** is not straightforward (Figure 12). As a matter of fact, the **8** molecule, of  $A''$  symmetry, has one unpaired electron in a  $\sigma$ -type OM (symmetry  $a'$ ) and one in the  $\pi$  allyl-type system (symmetry  $a''$ ) though mainly located on the carbon atom. The molecule has thus a short C1–O bond length, characteristic of a double bond. When the C2C1O angle decreases, this planar structure increases in energy and correlates with a high-energy state of dominant  $(\sigma_{\text{C2O}})^2$  ( $\sigma_{\text{C2O}}^*$ ) $^1$  configuration. On the contrary, the cyclic nonplanar molecule **11**, by opening of C2C1O, correlates with a nonplanar  $\pi\pi^*$  triplet located on C–C plus a C2 $\cdots$ O singlet diradical, with a long C1–O bond (ca. 1.43 Å). These two states reach the same energy for a C2C1O angle of ca.  $80^\circ$ . They are linked one to another by rotations of both C–H bonds around C–C: a sudden change of dominant configuration occurs during this movement resulting in the failing of all attempts to optimize the TS **12** using standard procedures. This structure was finally approximated from a grid of points performed at the MCSCF-(4,4)/6-31G\*\* level. The opening of cyclic **11** thus appears as a forbidden reaction, in agreement with the high frequency of the vibration associated to the CO breaking ( $897\text{ cm}^{-1}$ ) and the high energy barrier (29.4 kcal/mol at the CCSD(T)/cc-pVTZ level) along the **11**  $\rightarrow$  **8** process, as compared to the corresponding singlet **1**  $\rightarrow$  **3** transformation.

**Triplet Formylcarbene Isomerization into Triplet Ketene; Cyclic Triplet Ketene.** We considered the possible hydrogen transposition in formylcarbene **8** yielding triplet ketene **13**. The corresponding TS **14** is found at 50.6 kcal/mol and 45.0 kcal/mol above **8** at the respective UMP2 and CCSD(T) levels. The triplet ketene **13** lies at 19.5 kcal/mol (UMP2) and 20.4 kcal/mol (CCSD(T)) respectively below **8**. Structure **13** is planar, of  $A''$  symmetry; one unpaired electron is in the allyl-like  $\pi$  system, whereas the other one occupies a nonbonding  $a'$  MO in the molecular plane, mainly located on the carbon atom.

The geometry of the triplet carbene **15**, cyclic form of ketene **13**, has been optimized. The species **15** lies far above **13** (64.3 kcal/mol (UMP2) and 64.5 (CCSD(T)) but is nevertheless quite stable on the triplet PES; the frequencies associated to the opening of the cycle are greater than  $650\text{ cm}^{-1}$ . It is worthy to note that the triplet carbene **15** has a much higher energy than the corresponding singlet **6c**: 56.1 and 58.7 kcal/mol at the respective UMP2 and CCSD(T) levels. As a matter of fact, the typical equilibrium angle is ca.  $130^\circ$  in a triplet carbene vs ca.  $100^\circ$  in a singlet one, so that the triplet cycle **15** is much more

**TABLE 5: Energies of the C<sub>2</sub>H<sub>2</sub>O Triplet Species (Hartrees)<sup>a</sup>**

	UB3LYP <sup>b</sup>	UMP2 <sup>c</sup>	CCSD(T) <sup>d</sup>	MCSCF(8,7) <sup>e</sup>	MCSCF(12,12) <sup>f</sup>	MR-AQCC <sup>f</sup>
<b>8</b>	-152.48989	-152.11404	-152.23937	-151.77839		
<b>8t TS</b>		-152.10438	-152.22845			
<b>9</b>	-152.48739	-152.11240	-152.23740	-151.77687		
<b>10</b>	-152.44243	-152.06816	-152.19374	-151.71706		
<b>10S</b>	<i>-152.41494</i>		<i>-152.19159</i>	<i>-151.71948</i>		
<b>11</b>	-152.44275	-152.06925	-152.19443	-151.71753	-151.81170	152.17666
<b>11S</b>	<i>152.42034</i>		<i>-152.19277</i>	<i>-151.72114</i>	<i>-151.81071</i>	<i>-152.18220</i>
<b>12 TS</b>			-152.14683 <sup>g</sup>			
<b>13</b>		-152.14516	-152.27187			
<b>14 TS</b>		-152.03333	-152.16759			
<b>15</b>		-152.04268	-152.16911			

<sup>a</sup> Italics Refer to Vertical Singlet Energy (i.e. singlet state of same geometry). <sup>b</sup> 6-31G\*\*. <sup>c</sup> 6-311++G\*\*. <sup>d</sup> cc-PVTZ, MP2 geometries. <sup>e</sup> cc-PVTZ. <sup>f</sup> cc-PVTZ, MCSCF(8,7) geometry. <sup>g</sup> Geometry taken from a grid MCSCF(4,4)/6-31G\*\* (see text).

**TABLE 6: Calculated Geometries (Lengths in Angstroms, Angles in Degrees) of the C<sub>2</sub>H<sub>2</sub>O Triplet 8–12 Species<sup>a</sup>**

		C <sub>1</sub> C <sub>2</sub>	C <sub>1</sub> H <sub>1</sub>	C <sub>2</sub> H <sub>2</sub>	C <sub>1</sub> O	OC <sub>1</sub> C <sub>2</sub>	H <sub>1</sub> C <sub>1</sub> C <sub>2</sub>	C <sub>1</sub> C <sub>2</sub> H <sub>2</sub>	OC <sub>2</sub> C <sub>1</sub> H <sub>1</sub>	OC <sub>1</sub> C <sub>2</sub> H <sub>2</sub>
<b>8</b>	UDFT	1.418	1.103	1.087	1.242	119.5	118.8	129.0	180.0	0.0
	UMP2	1.468	1.108	1.085	1.190	122.3	115.1	129.1	180.0	0.0
	MCSCF	1.438	1.085	1.071	1.231	122.5	117.2	128.9	180.0	0.0
<b>8t TS</b>	UMP2	1.498	1.112	1.082	1.180	124.4	113.7	134.2	180.	91.1
	UDFT	1.417	1.116	1.086	1.234	126.1	113.5	132.04	180.0	180.0
<b>9</b>	UMP2	1.468	1.116	1.084	1.185	125.9	112.1	130.3	180.0	180.0
	MCSCF	1.440	1.089	1.071	1.227	123.5	116.4	129.6	180.0	180.0
	UDFT	1.436	1.091	1.091	1.407	60.0	134.4	134.4	101.6	-101.6
<b>10</b>	UMP2	1.435	1.087	1.087	1.405	59.3	134.5	134.5	101.6	-101.6
	MCSCF	1.419	1.074	1.074	1.414	59.9	134.3	134.3	102.9	-102.9
	UDFT	1.437	1.090	1.090	1.406	59.2	132.4	132.4	104.7	104.7
<b>11</b>	UMP2	1.436	1.086	1.086	1.404	59.3	131.2	131.2	104.7	104.7
	MCSCF	1.419	1.073	1.073	1.413	59.9	131.2	131.2	105.8	105.8
	MCSCF	1.501	1.081	1.071	1.305	80.8	120.2	132.9	121.9	-40.0

<sup>a</sup> See caption of Table 5.

**TABLE 7: Calculated Geometries (Lengths in Angstroms, Angles in Degrees) of the C<sub>2</sub>H<sub>2</sub>O Triplet 13–15 Species<sup>a</sup>**

		C <sub>1</sub> C <sub>2</sub>	C <sub>1</sub> H <sub>1</sub>	C <sub>1</sub> H <sub>2</sub>	C <sub>1</sub> O	C <sub>1</sub> C <sub>2</sub> O	H <sub>1</sub> C <sub>1</sub> C <sub>2</sub>	H <sub>2</sub> C <sub>1</sub> C <sub>2</sub>	H <sub>1</sub> C <sub>1</sub> C <sub>2</sub> O	H <sub>2</sub> C <sub>1</sub> C <sub>2</sub> O
<b>13</b>	UMP2	1.469	1.080	1.087	1.188	127.9	119.7	120.0	180.0	0.0
<b>14 TS</b>	UMP2	1.394	1.099	1.457	1.186	144.9	134.6	54.3	3.4	-131.4
<b>15</b>	UMP2	1.445	1.086	1.086	1.536	66.6	120.6	120.6	-96.9	96.9

<sup>a</sup> See caption of Table 5.

strained than the singlet one **6c**. At any rate, the formation of **15** is as unlikely as that of **6c** for similar reasons; in the TS **14**, the CCO angle is ca. 145°, close to its equilibrium value in the ketene **13** (ca. 128°).

**4.3. Singlet and Triplet Surfaces of the Oxirene–Formylcarbene System.** As far as, according to the preceding calculations, a possibility remains that oxirene **3** is not a minimum on the singlet surface while the couple **10–11** is quite stable on the triplet surface, the latter species could be a metastable state of oxirene. To answer this question, the vertical singlet energies of **10** and **11** (i.e., with the same geometry), referred to as **10S** and **11S**, were calculated at various levels. The corresponding results are reported in italics in Table 5. Indeed, the triplet energy of **11** is found below singlets **10S** and **11S** by ca. 14 kcal/mol at the UB3LYP level. This difference drops to 1.35 kcal/mol (**11–10S**), 1.05 kcal/mol (**11–11S**) at the CCSD(T) level, and to 0.92 kcal/mol (**11–11S**) at the MCSCF(12,12) one, which is near to the full valence active space of 16 electrons in 14 OM. By contrast, singlet **11S** is found more stable than **11** by 2.27 kcal/mol at the MCSCF(8,7) level and by 3.47 kcal/mol at the MR-AQCC one. We can only conclude that both singlet and triplet surfaces are very close to one another in this area of the PES. The situation is summarized in Figure 11: if **11** is more stable than **11S**, which would prevent a triplet–singlet crossing, this species, once formed, is likely to be trapped at a very low temperature. If, on the contrary, **11S** is below **11**, the

latter undergoes a fast intersystem crossing, spontaneously yielding singlet oxirene **3** and/or formylcarbene **1**.

The formylcarbene has clearly a triplet ground state, a point that has not been studied since 1978<sup>49</sup> until very recently.<sup>28</sup> At any level of calculation, the triplet species **8** is found at a lower energy than the singlet **1**. This calculated gap is of 7.85 kcal/mol (UB3LYP), 5.06 kcal/mol. (MR-AQCC), and 3.4 kcal/mol (CCSD(T)). The latter value is in good agreement to that of 3.59 kcal/mol reported by Scott et al.<sup>28</sup> at the W1' level (high calculation level based on CCSD(T) with extrapolation at infinite basis set and including ZPE correction). (Let us recall that singlet formylcarbene has not been found at the MP2/6-311++G\*\*<sup>28</sup>; at this level, the triplet formylcarbene **8** is 5.13 kcal/mol below the singlet oxirene **1**.) As a consequence, the singlet PES linking **1** and **3** crosses twice the triplet one. An easy intersystem crossing is thus expected along this path, finally yielding triplet **8** (or **9**). As far as Figure 12 is a realistic picture of reaction profiles, the reaction of oxygen atom, as well singlet as triplet, could easily end in the formation of **8** or **9**.

## 5. Concluding Remarks

The potential energy surfaces of the reactions of atomic oxygen O(<sup>1</sup>D) and O(<sup>3</sup>P) on acetylene C<sub>2</sub>H<sub>2</sub> at the UB3LYP/6-31G\*\* level appears to offer a good overview of the reactivity (except in the oxirene-formylcarbene area), as confirmed by further UMP2, CCSD(T), and MRCI calculations.

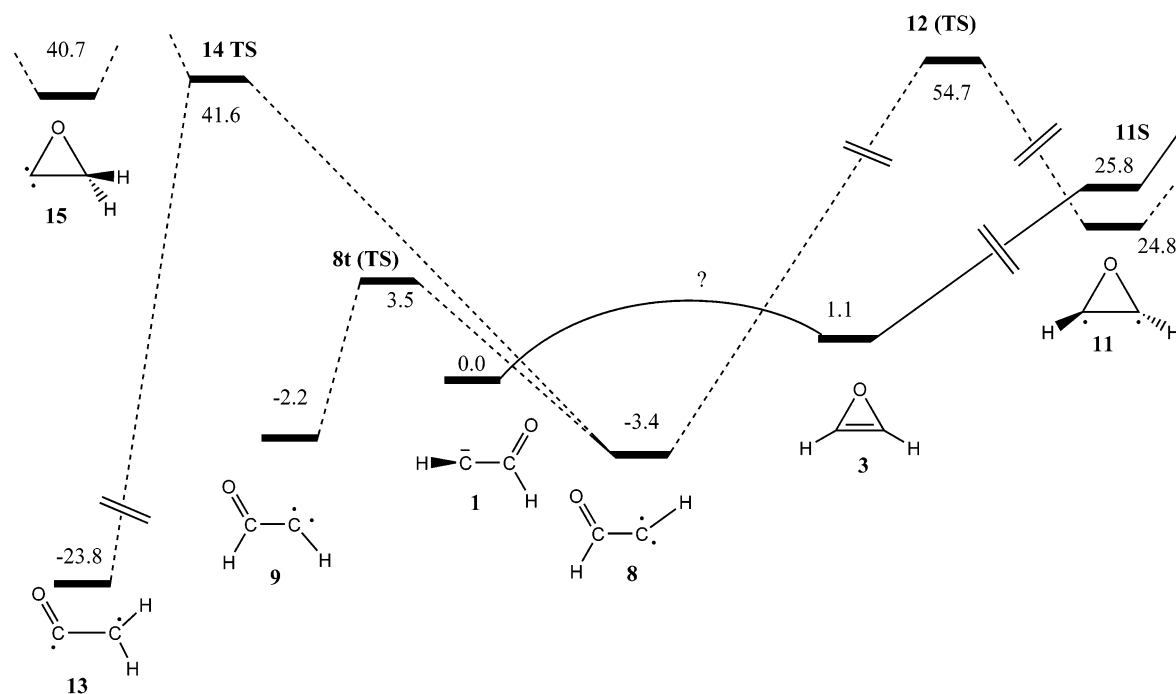


**Figure 11.** Energy profiles (kcal/mol) of triplet (dotted lines)  $\text{C}_2\text{H}_2\text{O}$  species interconversion and comparison with singlet (full lines) at the CCSD(T)/cc-pVTZ level. Note that the relative energies of **11** and **11S** may be inverted according to the calculation method (see text).

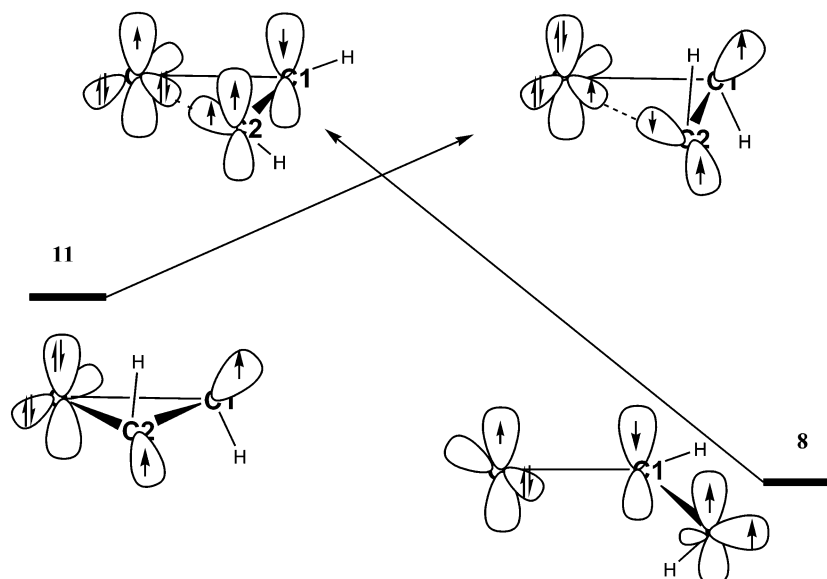


**Figure 12.** Main configurations involved in the interconversion of triplet oxirene **10** into triplet formylcarbene **8**.

Though we did not consider the secondary bond cleavage occurring in gas phase reactions, the PES of Figures 2 and 8 provide the main trends in these processes. Regarding the singlet one (Figure 2), we can expect the easy formation of ethynol transient with ca. 150 kcal internal energy possibly resulting in C–H, C–O, and O–H bond breaking and formation of H,  $\text{C}_2\text{OH}$ , OH,  $\text{HC}_2$ , and  $\text{HC}_2\text{O}$ . Because C–O is the weaker of these three bonds, OH and  $\text{HC}_2$  are expected to be the main products, in contrast to triplet reaction in which the process (hydrogen abstraction by oxygen) yielding these products is not important.<sup>19</sup>

If we now focus again on the inert matrix at very low-temperature conditions, let us first remark that, at 10 K, for example,  $RT = 0.02$  kcal/mol, which allows us to observe, as stable, compounds very reactive at room temperature. The main primary singlet product appears to be ethynol which is stable in these conditions. Nevertheless, the oxygen approach with

small  $\theta$  angles could lead to oxirene and/or formylcarbene which should be both observed if separated by an energy barrier of at least ca. 0.5 kcal/mol, as suggested by our higher level calculations and previous results.<sup>24</sup> A moderate raising in temperature would induce an intersystem crossing along the surface linking oxirene and formylcarbene finally yielding triplet formylcarbene.

The analysis of the triplet surface shows that the reaction is likely to end with a cis or trans triplet formylcarbene. Trapping the lowest triplet state of oxirene is another possibility, because, according to CCSD(T) calculation, the vertical singlet of this structure lies above the triplet one. Nevertheless, other calculations such as MR-AQCC predict the opposite result and thus a fast intersystem crossing toward singlet PES. In this case again, the formation of oxirene, if stable with respect to formylcarbene, is expected.



If singlet or triplet atomic oxygen is generated by ozone dissociation, we have to take into account the formation of a  $O_3-C_2H_2$  precursor complex, the structure of which may have a strong effect on the selectivity of subsequent reactions.<sup>56b</sup> Such a complex has already been studied,<sup>50–52,57</sup> and according to recent results,<sup>57</sup> a terminal oxygen atom is located at  $\theta = 20^\circ$  and  $r = 3.2 \text{ \AA}$ . This structure thus should favor small angle attacks of oxygen and thus the insertion into CC yielding oxirene and/or formylcarbene. Though the efficient competition of ethynol formation, such an experiment could be one of the rare possibilities to answer the question of the existence of oxirene.

Oxirene formation will be favored by suitable substituents R on acetylene, which could stabilize oxirene and make the insertion reaction into the C–R bond more difficult. To this end, the study of mono and difluoroacetylene substrates is in progress.

**Acknowledgment.** A great part of this work has been done thanks to the computational means supplied by the Centre de Calcul Recherche of the Pierre et Marie Curie University in Paris.

## References and Notes

- Hoffman, M. R.; Schatz, G. C. *J. Chem. Phys.* **2000**, *113*, 9456.
- Ramachandran, B.; Snekowitsch, J.; Wyatt Robert, E. *Chem. Phys. Lett.* **1997**, *270*, 387. Ramachandran, B.; Schrader, E. A. III; Senekowitsch, J.; Wyatt, R. E. *J. Chem. Phys.* **1999**, *111*, 3862.
- Wortmann-Saleh, D.; Engels, B.; Peyerimhoff, S. D. *J. Phys. Chem.* **1994**, *98*, 9541.
- Min, Z.; Wong, T.; Quandt, R.; Bersohn, R. *J. Phys. Chem. A* **1999**, *103*, 10451.
- Knyazev, V. F.; Arutyunov, V. S.; Vedenev, V. I. *Int. J. Chem. Kinetics* **1992**, *24*, 545.
- Hammond, B. L.; Huang, S. Y.; Lester, W. A., Jr.; Dupuis, M. J. *Phys. Chem.* **1990**, *94*, 7969.
- Ho, T.; Hollebeck, T.; Rabitz, H.; Harding, L. B.; Schatz, G. C. *J. Chem. Phys.* **1996**, *105*, 10472.
- Martinez, T.; Hernandez, M. L.; Alvario, J. M.; Lagan, A.; Aoiz, F. J.; Mendez, M.; Verdasco, E. *Phys. Chem. Chem. Phys.* **2000**, *2*, 589. Peterson, K. A.; Skokov, S.; Bowman, J. M. *J. Chem. Phys.* **1999**, *111*, 7445. Bitterova, M.; Bowman, J. M.; Peterson, K. *J. Chem. Phys.* **2000**, *113*, 6186.
- Last, I.; Aguilar, A.; Sayos, R.; Gonzalez, M.; Gilbert, M. *J. Phys. Chem. A* **1997**, *101*, 1206.
- Gonzales, M.; Troya, D.; Puyuelo, M. P.; Sayos, R.; Enriquez, P. A. *Chem. Phys. Lett.* **1999**, *300*, 603.
- Wada, S.; Obi, K. *J. Phys. Chem. A* **1998**, *102*, 3481.
- Arai, H.; Kato, S.; Koda, S. *J. Phys. Chem.* **1994**, *98*, 12.
- Tsurumaki, H.; Fujimura, Y.; Kajimoto, O. *Chem. Phys. Lett.* **1999**, *301*, 145.
- Kono, M.; Matsumi, Y. *J. Phys. Chem. A* **2001**, *105*, 65.
- Atkinson, R.; Baulch, D. L.; Cox, R. A.; Hampson, R. F.; Kerr, J. A.; Troe, J. *J. Phys. Chem. Ref. Data* **1992**, *21*, 1125.
- Atkinson, R.; Baulch, D. L.; Cox, R. A.; Hampson, R. F.; Kerr, J. A.; Rossi, M. J.; Troe, J. *J. Phys. Chem. Ref. Data* **1997**, *26*, 215.
- Brooke, T. Y.; Tokunaga, A. T.; Weaver, H. A.; Crovisier, J.; Brockelée-Morvan, D.; Crisp, D. *Nature* **1996**, *383*, 606.
- Peeters, J. *Bull. Soc. Chim. Belg.* **1997**, *106*, 337 and references therein. Peeters, J.; Boullart, W.; Langhans, I. *Int. J. Chem. Kinet.* **1994**, *26*, 869.
- Harding, L. B.; Wagner, A. F. *J. Phys. Chem.* **1986**, *90*, 2974.
- Boullart, W.; Peeters, J. *J. Phys. Chem.* **1992**, *96*, 9810.
- Huang, X.; Xing, G.; Bersohn, R. *J. Chem. Phys.* **1994**, *101*, 5818.
- Dykstra, C. E. *J. Chem. Phys.* **1978**, *68*, 4244.
- Tanaka, K.; Yoshimine, M. *J. Am. Chem. Soc.* **1980**, *102*, 7655.
- Scott, A. P.; Nobes, R. H.; Schaefer, H. F.; Radom, L. *J. Am. Chem. Soc.* **1994**, *116*, 10159.
- Gezelter, J. D.; Miller, W. H. *J. Chem. Phys.* **1995**, *103*, 7868.
- Smith, B. J.; Radom, L.; Kresge, A. J. *J. Am. Chem. Soc.* **1989**, *111*, 8297.
- Lewars, E.; Bonnycastle, I. *J. Mol. Struct.* **1997**, *418*, 17.
- Scott, A. P.; Platz, M. S.; Radom, L. *J. Am. Chem. Soc.* **2001**, *123*, 6069.
- Toscano, J. P.; Platz, M. S. *J. Am. Chem. Soc.* **1995**, *117*, 4712.
- Toscano, J. P.; Platz, M. S. *J. Am. Chem. Soc.* **1996**, *118*, 3527.
- Vacek, G.; Colegrove, B. T.; Schaefer, H. F. *Chem. Phys. Lett.* **1991**, *177*, 468.
- Vacek, G.; Galbraith, J. M.; Yamaguchi, Y.; Schaefer, H. F.; Nobes, R. H.; Scott, A. P.; Radom, L. *J. Phys. Chem.* **1994**, *98*, 8660.
- Fowler, J. E.; Galbraith, J. M.; Vacek, G.; Schaefer, H. F. *J. Am. Chem. Soc.* **1994**, *116*, 9311.
- (a) Becke, A. D. *J. Chem. Phys.* **1993**, *98*, 5648. (b) Lee, C.; Yang, W.; Parr, R. G. *Phys. Rev. B* **1988**, *37*, 785.
- Beno, B. R.; Fennen, J.; Houk, K. N.; Lindner, H. J.; Hafner, K. *J. Am. Chem. Soc.* **1998**, *120*, 10490.
- Raghavachari, K.; Trucks, G. W.; Pople, J. A.; Head-Gordon, M. *Chem. Phys. Lett.* **1989**, *157*, 479.
- Szalay, P. G.; Bartlett, R. J. *J. Chem. Phys.* **1995**, *103*, 3600.
- Szalay, P. G.; Bartlett, R. J. *Modern Ideas in Coupled-Cluster Methods*; Bartlett, R. J., Ed.; World Scientific: Singapore, 1997; p 81.
- Cremer, D.; Kraka, E.; Szalay P. G. *Chem. Phys. Lett.* **1998**, *292*, 97.
- (a) Woon, D. W.; Dunning, T. H. *J. Chem. Phys.* **1993**, *98*, 1358. (b) Kendall, R. A.; Dunning, T. H.; Harrison, R. J. *J. Chem. Phys.* **1992**, *96*, 6796.
- Frisch, M. J.; Trucks, G. W.; Schlegel, H. B.; Scuseria, G. E.; Robb, M. A.; Cheeseman, J. R.; Zakrzewski, V. G.; Montgomery, J. A., Jr.; Stratmann, R. E.; Burant, J. C.; Dapprich, S.; Millam, J. M.; Daniels, A. D.; Kudin, K. N.; Strain, M. C.; Farkas, O.; Tomasi, J.; Barone, V.; Cossi, M.; Cammi, R.; Mennucci, B.; Pomelli, C.; Adamo, C.; Clifford, S.; Ochterski, J.; Petersson, G. A.; Ayala, P. Y.; Cui, Q.; Morokuma, K.; Malick, D. K.; Rabuck, A. D.; Raghavachari, K.; Foresman, J. B.; Cioslowski, J.; Ortiz, J. V.; Stefanov, B. B.; Liu, G.; Liashenko, A.; Piskorz, P.; Komaromi, I.; Gomperts, R.; Martin, R. L.; Fox, D. J.; Keith, T.; Al-Laham, M. A.; Peng, C. Y.; Nanayakkara, A.; Gonzalez, C.; Challacombe, M.; Gill, P. M. W.; Johnson, B. G.; Chen, W.; Wong, M. W.; Andres, J. L.; Head-Gordon, M.; Replogle, E. S.; Pople, J. A. *Gaussian 98*, revision A.7; Gaussian, Inc.: Pittsburgh, PA, 1998.
- MCSCF/CASSCF: H.-J. Werner, P. J. Knowles, *J. Chem. Phys.* **1985**, *82*, 5053. Knowles, P. J.; Werner, H.-J. *Chem. Phys. Lett.* **1985**, *115*, 259. Werner, H.-J.; Meyer, W. *J. Chem. Phys.* **1980**, *73*, 2342. Werner, H.-J.; Meyer, W. *J. Chem. Phys.* **1981**, *74*, 5794. Werner, H.-J. *Adv. Chem. Phys.* **1987**, *69*, 1.
- Internally contracted MRCI: Werner, H.-J.; Knowles, P. J. *J. Chem. Phys.* **1988**, *89*, 5803. Knowles, P. J.; Werner, H.-J. *Chem. Phys. Lett.* **1988**, *145*, 514. Werner, H.-J.; Reinsch, E. A. *J. Chem. Phys.* **1982**, *76*, 3144. Werner, H.-J. *Adv. Chem. Phys.* **1987**, *69*, 1.
- Internally contracted MR-ACPF, QDVPT, MR-AQCC: Werner, H.-J.; Knowles, P. J. *Theor. Chim. Acta* **1990**, *78*, 175. Gdanitz, R. J.; Ahlrichs, R. *Chem. Phys. Lett.* **1988**, *143*, 413. Cave, R. J.; Davidson, E. R. *J. Chem. Phys.* **1988**, *89*, 6798. Szalay, P. G.; Bartlett, R. J. *Chem. Phys. Lett.* **1993**, *214*, 481.
- von Baar, B.; Weiske, T.; Terlouw, J. K.; Schwarz, H. *Angew. Chem., Int. Ed. Engl.* **1986**, *25*, 282.
- Hochstrasser, R.; Wirz, J. *Angew. Chem.* **1986**, *101*, 183.
- (a) Cszizmadia, I. G.; Font, J.; Strausz, O. P. *J. Am. Chem. Soc.* **1968**, *90*, 7360. (b) Thornton, D. E.; Gosavi, R. K.; Strausz, O. P. *J. Am. Chem. Soc.* **1970**, *92*, 1768. (c) Zeller, K. P. *Angew. Chem., Int. Ed. Engl.* **1977**, *11*, 781.
- Lewars, E. *J. Mol. Struct.* **1996**, *360*, 67.
- Baird, C.; Taylor, K. F. *J. Am. Chem. Soc.* **1978**, *100*, 1333.
- Gillies, J. Z.; Gillies, C. W.; Lovas, F. J.; Suenram, R. D.; Stahl, W. *J. Am. Chem. Soc.* **1989**, *111*, 3073.
- Gillies, J. Z.; Gillies, C. W.; Lovas, F. J.; Matsumura, K.; Suenram, R. D.; Kraka, E.; Cremer, D. *J. Am. Chem. Soc.* **1991**, *113*, 6408.
- Turi, L.; Dannenberg, J. J. *J. Phys. Chem.* **1993**, *97*, 7899.
- Lugez, C.; Schriver, A.; Levant, R.; Schriver-Mazzuoli, L. *Chem. Phys.* **1994**, *181*, 129.
- Moulin, V.; Schriver, A.; Schriver-Mazzuoli, L.; Chaquin, P.; *Chem. Phys. Lett.* **1996**, *263*, 423.
- Wrobel, R.; Sander, W.; Kraka, E.; Cremer, D. *J. Phys. Chem. A* **1999**, *103*, 3693.
- (a) Tevault, D. E.; Walker, N.; Smardzewski, R. R.; Fox, W. B. *J. Phys. Chem.* **1978**, *82*, 2733. (b) Bahou, M.; Schriver-Mazzuoli, L.; Schriver, A.; Chaquin, P. *Chem. Phys.* **1997**, *216*, 105. (c) Chaquin, P.; Alikhani, M. E.; Bahou, M.; Schriver-Mazzuoli, L.; Schriver, J. *Phys. Chem. A* **1998**, *102*, 8222.
- Cremer, D.; Kraka, E.; Crehuet, R.; Anglada, J.; Gräfenstein, J. *Chem. Phys. Lett.* **2001**, *347*, 268.